fishes

MDPI

Article

Broadband Characteristics of Target Strength of Pacific Chub Mackerel

Kohei Hasegawa [1,*], Naizheng Yan [1], Tohru Mukai [1], Yoshiaki Fukuda [2] and Jun Yamamoto [3]

[1] Faculty of Fisheries Sciences, Hokkaido University, Hakodate 0418611, Hokkaido, Japan; yan@fish.hokudai.ac.jp (N.Y.); mukai@fish.hokudai.ac.jp (T.M.)
[2] Fisheries Technology Institute, Japan Fisheries Research and Education Agency, Kamisu 3140408, Ibaraki, Japan; fukuda_yoshiaki03@fra.go.jp
[3] Field Science Center for Northern Biosphere, Hokkaido University, Hakodate 0418611, Hokkaido, Japan; yamaj@fish.hokudai.ac.jp
* Correspondence: kohase@fish.hokudai.ac.jp

Abstract: Broadband backscattering measurements of Pacific mackerel (*Scomber japonicus*) can improve acoustic surveys of the species for the management of its fisheries throughout the Pacific Ocean. The determination of its target strength (TS), the logarithmic form of the backscattering cross-section, is the aim of this work. It was measured for fourteen individual specimens, eight in a freshwater tank and six in a seawater tank, using calibrated broadband echosounders spanning the frequency band 24–84 kHz. The TS is expressed as a function of frequency and tilt angle, with fish length as a parameter. The individual broadband TS patterns with the tilt angle of fish showed size and frequency dependencies. The fish length-normalized TS of mackerel decreased with increasing fish length-to-acoustic wavelength ratio (l/λ) in the small l/λ range (approximately 2–6) but was flat in the larger l/λ range (>6). This variation in the normalized TS indicates that a pair of regression equations is necessary to span the range of commercially important mackerel relative to the acoustic wavelength. The relative l/λ characteristic of the normalized TS showed constant values with tilt-angle distributions over a large l/λ range and can be used as a characteristic of acoustic backscattering for discrimination among species.

Keywords: Pacific chub mackerel; broadband echosounder; fisheries resource management; acoustic discrimination

Key Contribution: This study investigated the target strength (TS) characteristics of Pacific chub mackerel. The results of ex situ measurements implied that the use of the fish length-to-wavelength ratio could show the dependence on fish size and frequency, as well as improve the determination of TS and the discrimination against other fish species.

check for updates

Academic Editor: Patrice Brehmer

Received: 6 January 2025
Revised: 23 January 2025
Accepted: 27 January 2025
Published: 28 January 2025

Citation: Hasegawa, K.; Yan, N.; Mukai, T.; Fukuda, Y.; Yamamoto, J. Broadband Characteristics of Target Strength of Pacific Chub Mackerel. *Fishes* **2025**, *10*, 51. https://doi.org/10.3390/fishes10020051

1. Introduction

In acoustic surveys for fisheries resource management, the acoustic backscattering characteristics of target species are key to correctly estimating abundance. Broadband echosounders using a frequency-modulated (FM) chirp signal provide a continuous frequency response of acoustic backscattering from a target that represents the characteristics of organisms, attributed to their morphological and size differences [1,2].

The genus *Scomber* is a group of small pelagic fish that are distributed globally [3]. The species of this group are an important fishery resource in several regions. The combined acoustic–trawl method, which obtains acoustic backscattering data with echosounders and

biological data from trawl catches, is commonly used to estimate fish biomass [4], and has also been used for stock assessments of *Scomber* spp. [5–7]. To estimate fish abundance using this method, the target strength in dB re. 1 m^2 (TS), which is the acoustic backscattering intensity from a single target, is essential for converting the volume backscattering coefficient into absolute fish densities [4]. The TS for estimating fish densities is usually derived from functions of fish length in cm, which is estimated from biological data as follows [8]:

$$TS = a\log_{10}l + b, \quad (1)$$

where a and b are the slope and intercept, respectively. TS is often assumed to be proportional to the square of l (i.e., $a = 20$) and is represented by the following:

$$TS = 20\log_{10}l + b_{20}. \quad (2)$$

Generally, the results of previous studies that investigated TS with respect to fish length were used to determine the coefficients of the function. However, the values of the coefficients used in some *Scomber* species are considered insufficient, owing to the lack of data on the TS of the group. A value of $b_{20} = -68.7$ at 38 kHz was used for surveys of the Atlantic chub mackerel, *S. colias* [7], and values of $a = -15.44$ and $b = 7.75$ (for estimating dB kg^{-1}) at 38 kHz were used for the Pacific chub mackerel, *S. japonicus* [6,9]. These values were estimated from another species of jack mackerel, *Trachurus murphyi* [10], and the Cape horse mackerel, *T. capensis* [11], respectively. Although the TSs of the genera *Scomber* and *Trachurus* are considered similar [12], the fish density estimated by the acoustic method greatly depends on TS and should be estimated based on the species concerned.

Pacific chub mackerel (hereafter referred to as mackerel) also play an important role as a fisheries resource worldwide. However, there is no appropriate reference for the TS of mackerel to estimate their densities using acoustic methods [6]. Although recent studies have estimated the TS of mackerel using an acoustic backscattering model [13–15] and tank experiment with free swimming fish [16], the b_{20} values estimated in these studies had a difference of 6–8 dB at various frequencies; the reason for this discrepancy is uncertain. As TS changes in a complicated manner, depending on multiple morphological and physiological factors, more studies are needed to accurately estimate the TS of mackerel. Specifically, the dependence of the TS on frequency is scarcely researched by measurements in situ or ex situ. Traditional single frequency echosounders provide discrete frequency data that are limited in information to understand the frequency dependence. The investigation of the relationships between the frequency response and other factors affecting the TS collected by broadband measurement may help to better understand the acoustic backscattering characteristics of mackerel. The idea of representing TS-normalized fish length as a function of the fish length-to-wavelength ratio (l/λ) was used to represent the size and frequency dependence of TS in two-dimensional graphs [17–19]. This representation has been used historically to summarize TS data obtained by discrete frequencies, fish length, and species [20–22]. The broadband acoustic measurement provides a specific relationship between TS and a wide l/λ range and may have an advantage in obtaining the general characteristics of acoustic backscattering for species. Yan et al. [23] used this idea to obtain the different TS characteristics among three fish species without swim bladders. In addition, the fish orientation, with respect to the incident angle of the acoustic signal, is also a critical factor affecting TS. The tilt-angle distribution of fish must be considered to determine the TS because the signal emitted from the echosounder hits the dorsal side of fish. The data on tilt-angle distribution in natural conditions are very scarcely measured but the standard deviation of it is close to 15° in general [21].

The frequency response of acoustic backscattering is also expected to enhance the acoustic discrimination among species [24,25]. As mackerel is widely distributed, not only horizontally but also vertically [26], overlaps between its distribution and that of other pelagic species can frequently occur. Therefore, the findings on the broadband backscattering of mackerel will also be useful for acoustic discrimination. The relative l/λ TSs represent the acoustic backscattering characteristics [27]. This idea is based on the relative frequency response, which is defined as the ratio of the target strength at a frequency to a reference frequency [28]. The relative frequency response of discrete multi-frequency can represent differences in backscattering characteristics among species groups, but it is difficult to discriminate among species that have similar frequency responses, such as swim bladder fish species [29,30]. The potential for discrimination among swim bladder fish species using the broadband frequency response remains a challenge in this field. The relative l/λ characteristic can represent the frequency and fish length dependence of acoustic backscattering, and it may improve the quality of acoustic discrimination [27].

The objective of this study was to derive the dependence of the TS of mackerel on the parameters of frequency, fish length, and tilt angle of fish. The measurements were conducted in experimental tanks to measure the dorsal-aspect TS patterns of mackerel related to the tilt angle by broadband frequency, and the results were compared with the modeled values. Additionally, we suggest the use of l/λ characteristics for estimating the TS of mackerel and for acoustic discrimination among species.

2. Materials and Methods

2.1. Fish Samples for Measurements

The mackerel used for the TS measurements were caught by angling in the coastal area around Hakodate, Japan, from July to October 2021. The fish samples were kept in two cylindrical tanks (a 2.6 m diameter × 0.9 m high tank, and a 1.8 m diameter × 0.6 m high tank) until measurement. The water temperature and the salinity of the two tanks were maintained at approximately 20 °C and 33 psu, respectively. Frozen krill was supplied to the fish as food once every two days. A total of 14 individuals, which were 14.8–23.4 cm in fork length (FL), were used for the measurements (Table 1). In this paper, fork length was used as the length of the mackerel and "l" was assigned as the variable.

Table 1. Morphological information of Pacific chub mackerel used in this study, range of l/λ, and measurement location and date.

No.	Fork Length (cm)	Swim Bladder Length (cm)	Swim Bladder Angle (°)	l/λ	Location	Date
1	15.5	4.3	11	2.5–7.2	HU	30 August 2021
2	21.2	6.1	9	3.4–9.8		30 August 2021
3	19.4	5.5	6	3.1–9.0		1 September 2021
4	14.8	4.0	8	2.4–6.8		1 September 2021
5	16.2	4.4	8	2.6–7.5		2 September 2021
6	23.0	7.1	6	3.7–10.6		2 September 2021
7	23.4	6.5	9	3.8–10.8		3 September 2021
8	15.6	4.2	11	2.5–7.2		3 September 2021
9	22.9	6.7	10	7.0–12.6	HRCFO	4 August 2021
10	23.4	5.2	9	7.2–12.8		5 August 2021
11	14.9	3.8	8	4.6–8.3		23 October 2021
12	22.7	5.0	9	7.1–12.6		23 October 2021
13	18.2	4.4	7	5.7–10.1		24 October 2021
14	15.9	3.8	13	4.9–8.8		24 October 2021

2.2. Design of Measurements in Experimental Tanks

The TS measurements of each mackerel were conducted in two experimental tanks: a 5 m × 5 m × 5 m freshwater tank, located at Hokkaido University (HU), and a

5 m × 10 m × 6 m saltwater tank at the Hakodate Research Center for Fisheries and Oceans (HRCFO). Eight individuals were measured at the former from 30 August to 3 September in 2021, and the others were measured at the latter from 4 to 5 August and 23 to 24 October in 2021 (Table 1).

For the measurements at HU, a bistatic custom-made broadband system based on that described by Amakasu et al. [31] was used. Two single-beam transducers were deployed at a depth of 2.5 m near the wall of the tank so that the acoustic signals were transmitted horizontally (Figure 1). The beam width of the transducers is 40° at 30 kHz and 17° at 70 kHz. Linear FM chirp pulses sweeping 20–70 kHz for 2 ms were generated with a function generator (WF1946, NF, Kanagawa, Japan), amplified by a power amplifier (PRO-50, Accuphase, Kanagawa, Japan), and applied to the transducer for transmission. Echoes from a target were detected by the receiving transducer, amplified by a differential preamplifier (LI-75A, NF, Kanagawa, Japan), and the received signal was recorded by an oscilloscope (WaveJet312A, Teledyne LeCroy, New York, NY, USA). The sampling rate of the recording was set to 20 MHz.

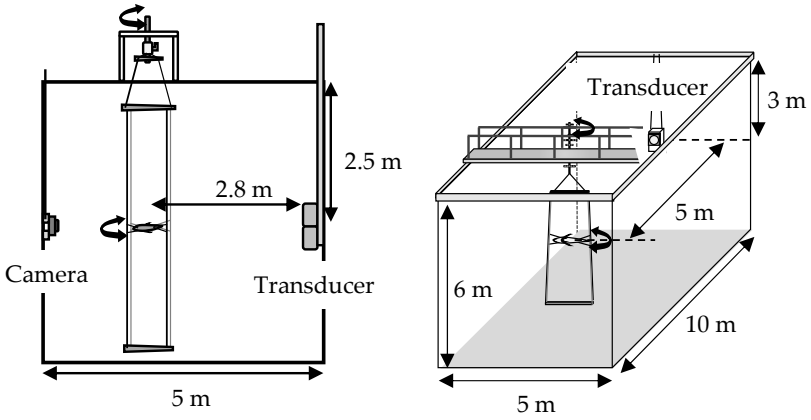

Figure 1. Deployments of measurement systems in the freshwater tank located at HU (**left**) and saltwater tank at HRCFO (**right**).

For the measurements at HRCFO, a Simrad EK80 echosounder system (Kongsberg Maritime, Kongsberg, Norway) consisting of a wideband transceiver (WBT) and a split-beam transducer (ES70-7C) was used. The transducer was placed in a box-shaped frame and deployed at a depth of 3 m (Figure 1). FM chirp pulses of 45–90 kHz, a 2.048 ms long duration, and a fast-ramping mode [32] were transmitted from the transducer horizontally, and echoes from the target were recorded using Simrad EK80 software (ver. 2.0.1).

Each mackerel was suspended in an experimental tank after being anesthetized with eugenol (FA100, Sumitomo Pharma Animal Health, Osaka, Japan). Four monofilament nylon fishing lines (0.15 mm in diameter) were used to suspend each mackerel in the water, by connecting a suspension system consisting of two flames connected by four multifilament polyethylene fishing lines (0.70 mm in diameter), so that the dorsal side of the fish could face the transducers. The fish were suspended at a distance of 2.8 m (tank in HU) and 5.0 m (tank in HRCFO) from the transducer. The suspended position was out of the near field of the transducer; it was at a distance from which the fish body can be assumed as a point target, and fish was within the first Fresnel zone [33]. All activities, from the anesthetic to the suspension procedure, were carefully conducted with the fish in water to prevent air bubbles from attaching to their bodies. The incident angle of the acoustic pulse was adjusted manually by rotating the suspension system. The echo from each mackerel was measured in the angle range of −40° to +40° in increments of 1° (the plus degree indicates the fish's head was pointed up towards the transducer). For each

angle, a waveform averaging eight pings was recorded in the measurement at HU, and more than ten ping echoes were recorded in the measurements at HRCFO.

2.3. Calibration of Echosounder Systems

Each system was calibrated using standard spheres made of tungsten carbide with 6% cobalt binder. Each sphere was suspended in a net bag made from monofilament nylon line (0.4 mm in diameter), according to Foote et al. [34]. The available frequency range of each system was evaluated by calibration.

A 38.1 mm diameter sphere was used for the calibration of the custom-made system. As the single-beam system could not measure the direction of the target, the position where the received echo level of the sphere was at its maximum at a frequency of 70 kHz was assumed to be on the beam axis of the transmitter and receiver transducers. After the echoes of the sphere were collected, echoes of another 22.2 mm diameter sphere were recorded at the same position as the 38.1 mm diameter sphere to confirm the calibration results using the following method. Each mackerel was suspended in the same position as the spheres by observing their position using a digital camera (TG-4, Olympus, Tokyo, Japan) deployed in the tank.

The EK80 system was calibrated using its calibration mode and a 25.0 mm diameter sphere. The echo data of the sphere were recorded until the center coverage, and the overall coverage was more than 80%, as displayed in the calibration mode. After recording, the outliers were removed manually using the software, and the parameters were updated.

2.4. Processing of Acoustic Data

The acoustic data from the custom-made system were recorded as time-series voltage waveforms received by the system. The Fourier transformation of the voltage $V_r(f)$ is defined by the following equation [31]:

$$V_r(f) = V_t(f)S_t(f)S_r(f)G(f)D(f)L(f)F_{bs}(f), \quad (3)$$

where f is the frequency (Hz), $S_t(f)$ and $S_r(f)$ are the system responses of the transmitter and receiver transducers, respectively, $D(f)$ is the directivity of the combination of the transmitter and receiver transducers, $G(f)$ is the system gain, $L(f)$ is the two-way acoustic attenuation, and F_{bs} is the backscattering amplitude of the target. The response of the entire system is defined as follows:

$$K(f) = \frac{V_r(f)}{L(f)F_{bs}(f)}, \quad (4)$$

A matched filter for processing the cross-correlation was applied to the recorded signals to increase the signal-to-noise ratio [35,36]. The compressed pulse $cp(t)$ is given by the cross-correlation between the received voltage $v_r(t)$ and replica $v_{rep}(t)$, which was defined as the signal applied to the transmitter transducer in this study, as follows [2,37]:

$$cp(t) = R_{rep}^{-1}(0)v_t(t) \otimes v_{rep}(t), \quad (5)$$

$$R_{rep}(t) = v_{rep}(t) \otimes v_{rep}(t), \quad (6)$$

where the term $\otimes$ denotes the correlation and $R_{rep}(t)$ represents the output of the autocorrelation between the replicas, which reaches a maximum value when the time lag of the two signals is zero ($t = 0$). The system response associated with the compressed pulse $K_{cp}(f)$ is given by

$$K_{cp}(f) = \frac{CP^*(f)}{L(f)F_{bs}(f)}, \quad (7)$$

where $CP(f)$ is the Fourier transformation of the compressed pulse and the superscript * denotes the complex conjugate. Then, the backscattering amplitude of the target and target strength is given by

$$F_{bs}(f) = \frac{CP^*_{tar}(f)}{K_{cp}(f)L(f)}, \quad (8)$$

$$TS(f) = 10\log|F_{bs}(f)|, \quad (9)$$

$K_{cp}(f)$ was derived from the calibration with a 38.1 mm standard sphere and the result was evaluated by comparing the measured and predicted $F_{bs}(f)$ of a 22.2 mm standard sphere. In this study, the compressed pulse was not tapered for Fourier transformation to ensure that the available bandwidth was as wide as possible [25]. A 250 µs long rectangular window was applied to calculate the spectrum of the compressed pulse (Figure 2).

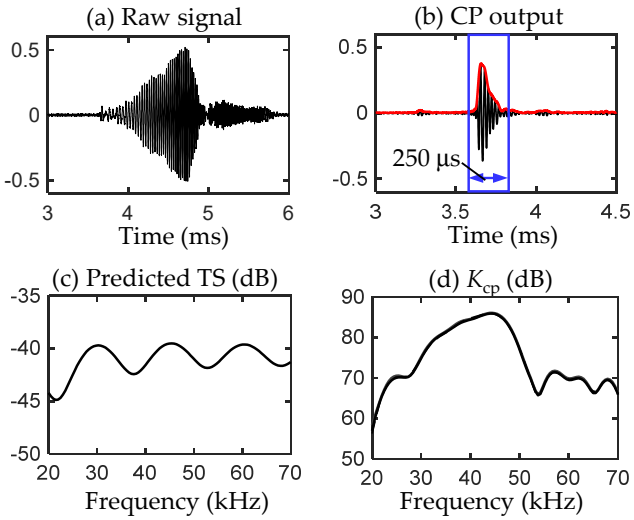

Figure 2. Analysis of calibration of 38.1 mm-diameter standard sphere with time-series single pulse. (**a**) Single echo received from the sphere; (**b**) output of the matched filter applied to the signal in (**a**); (**c**) predicted frequency response of TS for the sphere; (**d**) results of calculating the system response $K_{cp}(f)$, noting that the graph shows all results for K_{cp} measured on 23 August, 27 August, and 2 September, although the lines are almost overlapped.

The acoustic data recorded by the EK80 were processed using Echoview ver. 10.0.271 (Echoview Software, Hobert, TAS, Australia). The TS spectrum of the target was calculated using a single target detection (wideband) algorithm. The configuration of the algorithm parameters is listed in Table 2. For each incident angle, the spectrum of the TS calculated for all the pings was averaged on a linear scale.

Table 2. Parameters used in the single target detection algorithm of Echoview.

Parameter	Value
Compensated TS threshold (dB)	−90
Maximum beam compensation (dB)	6.0
Pulse length determination level (dB)	6.0
Minimum normalized pulse length	0.5
Maximum normalized pulse length	1.5
Window size (m)	0.4

2.5. Target Strength Estimated by Acoustic Backscattering Model

The Kirchhoff Ray Mode (KRM) backscattering model [38,39] was used to estimate the TS of the mackerel. The model assumes that the fish body is a series of fluid-like cylinders, and that the swim bladder is a series of gas-filled cylinders. The backscattering amplitude

from the whole body of the fish is calculated by summing the backscattering amplitudes from the fish body and the swim bladder coherently (see Clay and Horne [38] for a detailed derivation). The coordinates of the fish body and swim bladder were traced from X-ray photographs taken after the measurements using a radiographic instrument (SOFTEX CMB-2, SOXTEX Co., Ltd., Tokyo, Japan) (Figure 3). The photographs were scanned, and the shapes of the body and swim bladder were traced. The body of the fish was traced, except for the fins and tail. The traced images were rotated, so that the anteroposterior axis of the fish body was horizontal (i.e., on the x-axis), and digitized in increments of 1 mm along the x-axis. The acoustic parameters of the fish body, swim bladder, and water are listed in Table 3. The fish body and swim bladder parameters were obtained from Clay and Horne [38]. The sound speeds of water were calculated by Medwin [40] for freshwater and Mackenzie [41] for saltwater, based on the temperature, salinity, and depth of the fish in the tank experiments. Water densities of 1000 kg m^{-3} and 1025 kg m^{-3} were used for freshwater and saltwater, respectively. The frequency range used in the model was 20–90 kHz. The $TS(f)$ of each mackerel was predicted in a tilt-angle range of $-40°$ to $+40°$ in increments of 0.5°.

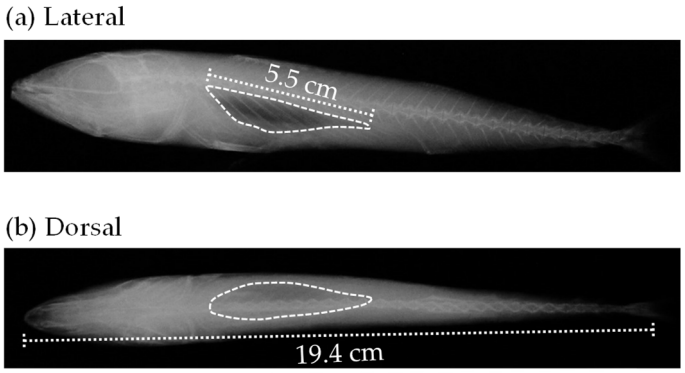

Figure 3. Radiographs of mackerel (No. 3 in Table 1) radiated to the lateral-aspect (**a**) and dorsal-aspect (**b**). The white dotted lines show the shape of the swim bladder.

Table 3. Parameters used in KRM model.

Parameter	No. 1–8	No. 9–10	No. 11–14
Sound speed in water (m s^{-1})	1492	1530	1513
Sound speed in fish body (m s^{-1})	1570	1570	1570
Sound speed in swim bladder (m s^{-1})	345	345	345
Density of water (kg m^{-3})	1000	1025	1025
Density of fish body (kg m^{-3})	1070	1070	1070
Density of swim bladder (kg m^{-3})	1.24	1.24	1.24

The length and angle of the swim bladders were also measured by X-ray photos viewed from lateral. The length between the front and end edge of the swim bladder was determined as the swim bladder length. The angle between the x-axis of the image and the line used to measure the swim bladder length was defined as the swim bladder angle.

2.6. Target Strength Representation

The TS pattern related to the tilt angle θ was averaged following the approach of Foote [42] for each frequency, assuming that the probability distribution of the angle was Gaussian:

$$TS(f)_{ave} = 10\log\left\{\frac{\int_{-40}^{40}\sigma_{bs}(f,\theta)g(\theta)d\theta}{\int_{-40}^{40}g(\theta)d\theta}\right\}, \quad (10)$$

where $\sigma_{bs}(f, \theta)$ is the backscattering cross-section in square meters, and $g(\theta)$ is the function for the tilt-angle distribution of fish, defined by

$$g(\theta) = \frac{1}{\sqrt{2\pi s^2}} \exp\left\{-\frac{(\theta - m)^2}{2s^2}\right\}, \quad (11)$$

where m and s are the mean and standard deviation of the distribution, respectively. To evaluate the dependence of the distribution on the tilt-averaged TS, four combinations of the m and s of Gaussian, $(m, s) = (-5, 10)$, $(-5, 15)$, $(0, 10)$, and $(0, 15)$, were used to calculate $TS(f)_{ave}$. The slope and the intercepts of Equations (1) and (2) were estimated from the $TS(f)_{ave}$ results for each tilt-angle distribution.

In addition to the regression using Equations (1) and (2), the TS related to l/λ was used to represent the specific characteristics of the acoustic backscattering of the mackerel. Backscattering cross-sections of the fish were normalized by fish length to compare the individual results with non-dimensional values. The regression equations for the normalized backscattering cross-section are as follows [19]:

$$10 \log \frac{\sigma_{bs}(l/\lambda)}{l^2} = \beta_1 \log \frac{l}{\lambda} + \beta_0, \quad (12)$$

$$TS_{norm} = 10 \log \frac{\sigma_{bs}}{l^2}, \quad (13)$$

where TS_{norm} is the normalized TS by the square of fish length. The average TS derived from Equation (10) for each angle distribution was used to calculate the normalized TS. The acoustic wavelength was calculated from the sound speed of each water tank and the frequency in increments of 1 kHz.

The relative TS normalized by fish length for l/λ was calculated by [27]

$$r\left(\frac{l}{\lambda}\right) = TS_{norm}\left(\frac{l}{\lambda}\right) - TS_{norm}\left\{\left(\frac{l}{\lambda}\right)_0\right\}, \quad (14)$$

where r is the relative TS normalized by fish length and $(l/\lambda)_0$ is the reference l/λ. $r(l/\lambda)$ was calculated in the case of $(l/\lambda)_0 = 7.1$, according to the range of each l/λ for the individual fishes (Table 1). However, the l/λ of two fish could not be within the range (No. 4 and No. 10), and the two were excluded from the analysis.

3. Results

3.1. Calibration Results and Frequency Bands for Analyses

The calibration of the custom-made system was performed three times, and the system response K_{cp} was stable (Figure 2). The predicted and measured TSs of the 22.2 mm diameter sphere were compared, and the results showed good consistency (within a 0.5 dB difference) at most frequencies (Figure 4). The difference was larger in some frequency ranges, where K_{cp} was relatively lower. Therefore, the frequency ranges (20–23, 52–54, 64–66, and 69–70 kHz) in which K_{cp} was less than 68 dB were judged as having a low signal-to-noise ratio and removed from the analyses.

The calibration results of the Simrad EK80 echosounder system with a split-beam transducer (ES70-7C) showed that the gain of the system was almost stable for each measurement in August and October, with a difference of up to 0.9 dB, except in the range of 45–47 kHz and 84–90 kHz (Figure 5). The data obtained in these frequency ranges were likely to be insufficiently accurate and were removed from the analyses.

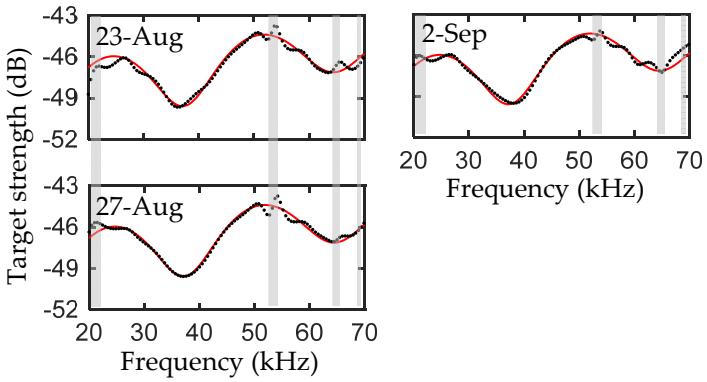

Figure 4. Frequency responses of the TS for a 22.2 mm diameter sphere. The dot marks show the TS measured by using a calibrated custom-made echosounder, and the solid lines show the predicted TS. The shaded frequency bands are excluded from the analyses due to a low signal-to-noise ratio.

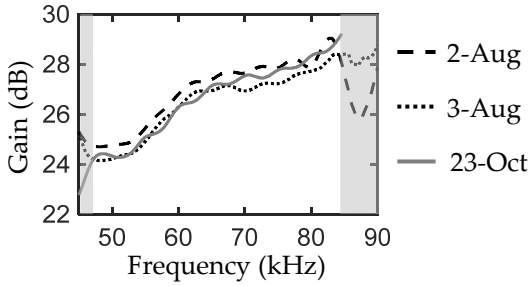

Figure 5. Gain of the EK80 system resulting from the calibration in the saltwater tank in August (black lines) and October (gray line). The shaded frequency bands are excluded from the analyses due to a large deviation in the gain.

3.2. Target Strength Pattern with Respect to Tilt Angle

The broadband TS patterns related to the tilt angle were obtained by tank measurements and modeled by KRM (Figures 6 and 7). The TS patterns were more complex at higher frequencies, including sharp peaks, lobes, and dips. Size dependence was also observed, as the larger samples had a relatively larger TS and slightly sharper peaks than the smaller ones. Similar TS patterns were observed between the measured and modeled results, but the peaks of the modeled TS tended to be broader than the measured TS. The TS patterns had an offset with respect to the tilt angle and the peak of TS appeared to be less than 0°. At higher frequencies, the peak was observed at an angle of approximately $-10°$ to $-5°$, which was a larger offset than that at lower frequencies. As the TS of the fish body was significantly lower than that of the swim bladder (Figure 8), the whole TS patterns were strongly affected by the swim bladder and the peak of TS generally appeared to correspond to the swim bladder angle relative to the body axis, as shown (Table 1). However, the modeled results also showed that the peak of the TS for the fish body near 0° was relatively large at some frequency ranges, which was enough to affect the entire TS pattern. In the lower-frequency band, the width of the peak was relatively variable with respect to the frequency.

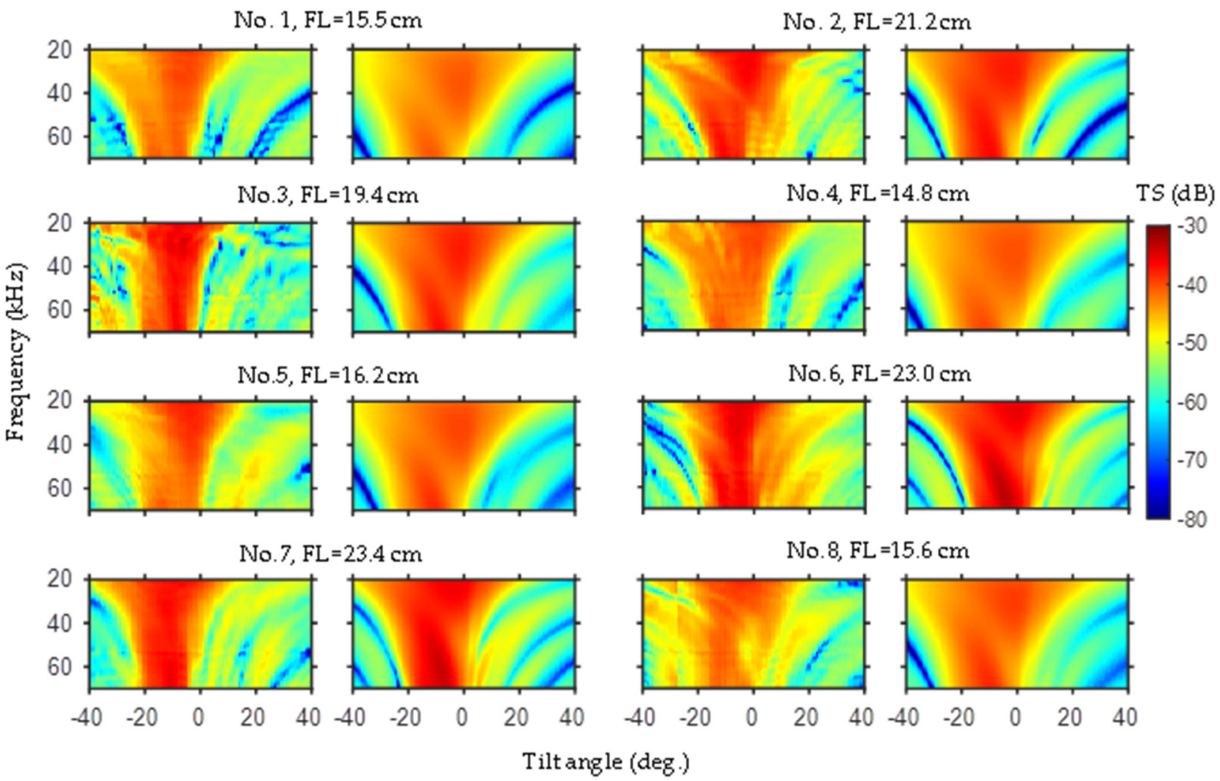

Figure 6. Individual TS patterns with respect to tilt angle (−40 to +40 degrees) and frequency (20 to 70 kHz) measured with a custom-made system (left of each pair of panels) and modeled by the Kirchhoff ray mode model (right of each pair of panels). The measured TS included the data removed from the analyses due to a low signal-to-noise-ratio. For the tilt angle, the plus degree means the fish's head was pointed up towards the transducer.

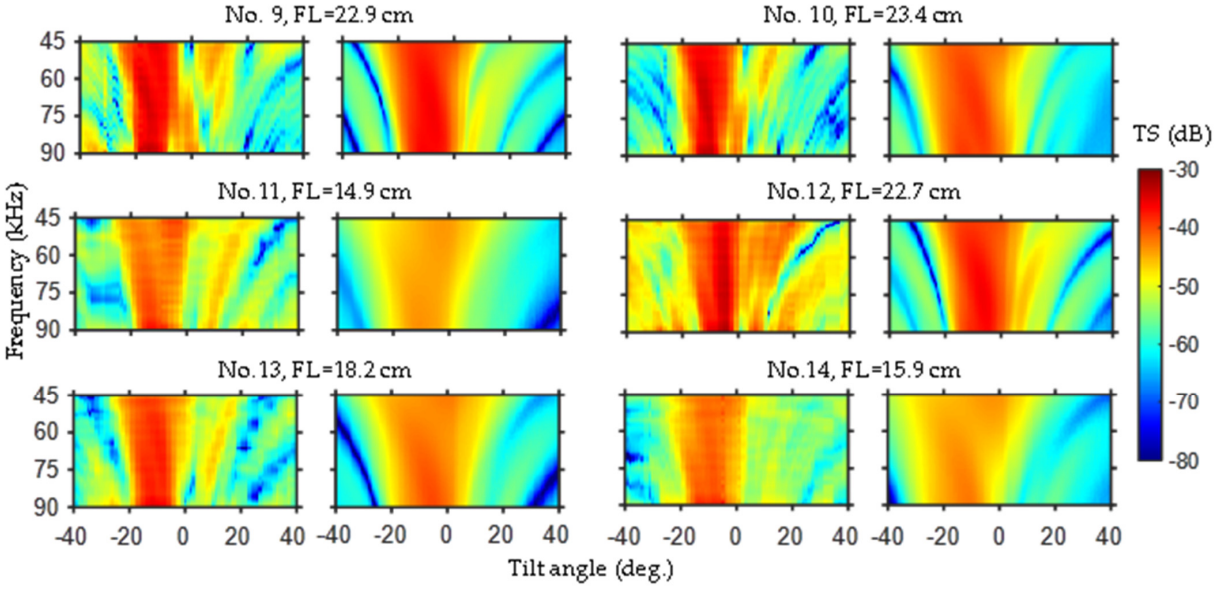

Figure 7. Individual TS patterns with respect to tilt angle (−40 to +40 degrees) and frequency (45 to 90 kHz) measured with the EK80 system (left of each pair of panels) and modeled by the Kirchhoff ray mode model (right of each pair of panels). The measured TS included the data removed from the analyses due to the unstable gain of the system, shown by the results of the calibration (Figure 5).

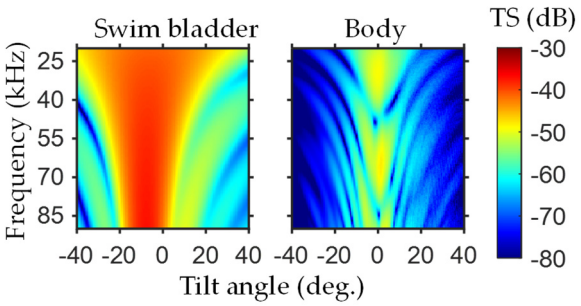

Figure 8. TS pattern of sample No. 3 (FL = 19.4 cm) predicted by the Kirchhoff ray mode model for swim bladder (left panel) and fish body (right panel). The frequency range is 20 to 90 kHz.

3.3. Target Strength Related to Fish Length

The average TS was calculated using four tilt-angle distributions, and the regression lines related to the fork length in cm at discrete frequencies of 38 kHz, 50 kHz, and 70 kHz are listed in Table 4. The coefficient of b_{20} agreed between the measured and modeled values within a difference of 0.3 dB. The b_{20} was highest at the three frequencies when the tilt-angle distribution was assumed to be (−5, 10) and lowest when it was assumed to be (0, 15). The difference in b_{20} was 1.4–1.7 dB between the two tilt-angle distributions. The data obtained at 50 kHz showed no discrepancy between the results from the two systems. The slope a of the regression line did not vary noticeably with the tilt-angle distribution at any frequency. However, the slope and intercept of the regression calculated over the frequency band showed that the coefficients varied significantly with frequency (Figure 9). The slope a and intercept b of the measured TS agreed with those of the modeled TS at frequencies higher than 40 kHz, while the values exhibited large differences at the lower frequency. The coefficients calculated from the modeled TS were more variable with the tilt-angle distribution than the measured TS. The values of b_{20} decreased slightly with the increase in frequency.

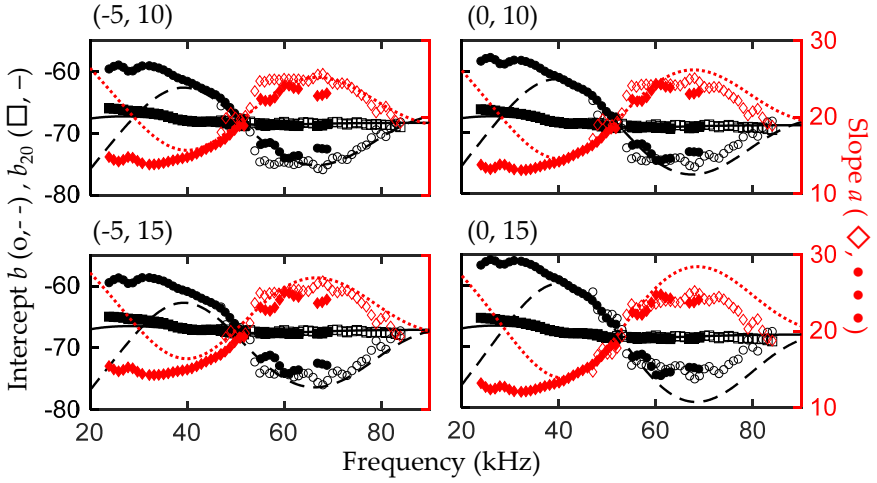

Figure 9. Coefficients of the regression equation between TS and fish length related to frequency. Each panel shows the result for the coefficient of slope a and intercept b or b_{20} by changing the tilt-angle distribution. The data calculated from the measured TS were plotted according to their source, i.e., custom-made system (solid markers) and EK80 system (open markers), including the overlapping frequency range. For the measured data, slope a is shown by diamonds, intercept b is shown by circles, and b_{20} is shown by squares. The solid line shows b_{20}, the dotted line shows slope a, and the dashed lines show intercept b, calculated from the modeled TS.

Table 4. The coefficients of the regression equations calculated from the relationship between the target strength and fish length (cm) by tilt-angle distributions.

System	Frequency (kHz)	(−5, 10)			(−5, 15)			(0, 10)			(0, 15)		
		a	*b*	b_{20}	*a*	*b*	b_{20}	*a*	*b*	b_{20}	*a*	*b*	b_{20}
Custom	38	15.0	−60.4	−66.7	14.7	−61.0	−67.7	12.9	−58.5	−67.4	13.9	−60.4	−68.1
Model		16.8	−62.8	−66.9	16.0	−62.7	−67.8	14.3	−60.0	−67.3	14.8	−61.4	−68.1
Custom	50	18.7	−66.1	−67.7	18.5	−66.7	−68.7	17.4	−65.3	−68.6	18.0	−66.6	−69.1
EK80		19.4	−66.8	−67.6	20.1	−68.6	−68.5	17.0	−64.7	−68.6	19.1	−67.8	−69.0
Custom and EK80		19.2	−66.5	−67.6	19.3	−67.7	−68.6	17.3	−65.1	−68.6	18.6	−67.3	−69.1
Model		20.3	−67.9	−67.5	19.1	−67.3	−68.5	17.9	−65.6	−68.3	18.3	−66.8	−68.9
EK80	70	25.4	−74.1	−67.1	24.5	−74.0	−68.2	24.2	−73.7	−68.3	24.0	−73.9	−68.8
Model		26.8	−75.9	−67.3	25.0	−74.8	−68.4	28.4	−79.0	−68.3	26.0	−76.6	−69.0

3.4. Fish Length-to-Wavelength Ratio Characteristics

The TS normalized by fish length or acoustic wavelength were calculated using each tilt-angle distribution. The l/λ characteristics of the normalized TS were dependent on size and frequency (Figures 10 and 11). The fish length-normalized TS showed an obvious change in characteristics at approximately l/λ = 6, and the single regression lines of Equation (12) did not explain the entire characteristic (the determination coefficient R^2 was between 0.32 and 0.42 for each tilt-angle distribution). Then, a pair of lines was derived such that the residual error was the lowest (Table 5). The boundaries of the lines were in the range of l/λ = 6.1–6.3 for the four tilt-angle distributions. A difference in the normalized TS among the tilt-angle distributions was observed.

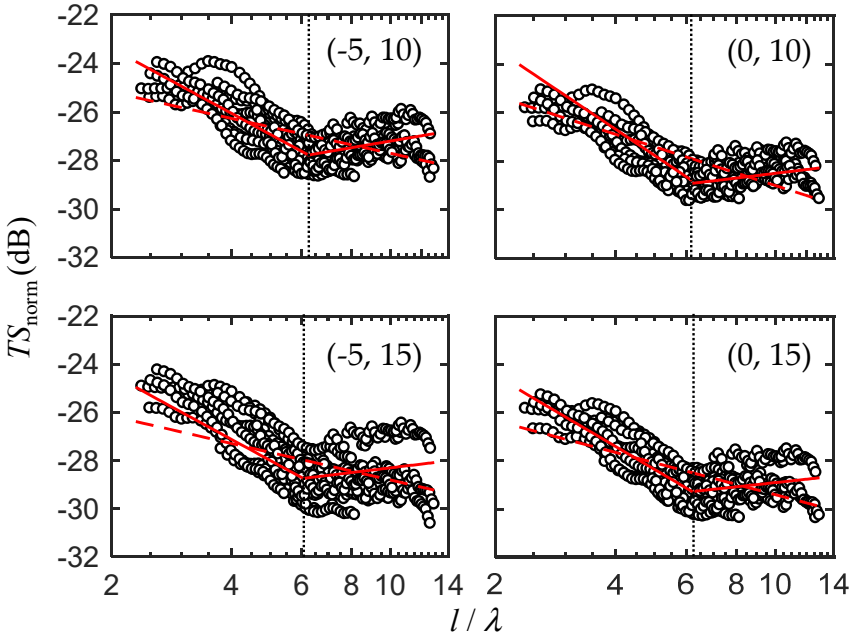

Figure 10. Fish length-normalized TS related to the fish length-to-wavelength ratio calculated from the measured results of individual fish (circles). Each panel shows the difference in tilt-angle distribution. The red lines show the regression lines obtained from all of the data (dashed lines) and from divided data, so that the residual sum of squares was at its minimum (solid lines). The dot lines show the boundary of the two regression lines of the divided data.

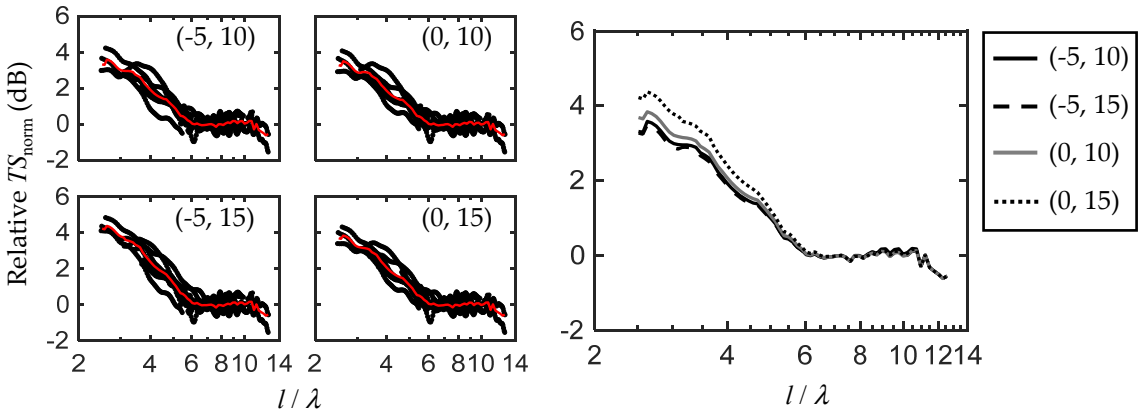

Figure 11. Relative TS normalized by fish length related to fish length-to-wavelength ratio. The four left panels show the relative TS_{norm} calculated from the data of individual fish (black circles) and the averaged values (solid red lines). The right panel shows each averaged data (lines in left panels) on a graph.

Table 5. Equations of TS as a function of fish length and acoustic wavelength by tilt-angle distribution.

Tilt-Angle Distribution	Equation for TS	Range of l/λ	Residual Sum of Squares
(−5, 10)	$16.4 \log l + 3.6 \log \lambda - 24.1$	$2.4 < l/\lambda < 12.8$	4.1
	$11.1 \log l + 8.9 \log \lambda - 20.7$	$2.4 < l/\lambda \leq 6.2$	2.5
	$22.8 \log l - 2.8 \log \lambda - 30.0$	$6.2 \leq l/\lambda < 12.8$	
(−5, 15)	$16.2 \log l + 3.8 \log \lambda - 25.0$	$2.4 < l/\lambda < 12.8$	3.3
	$11.0 \log l + 9.0 \log \lambda - 21.7$	$2.4 < l/\lambda \leq 6.1$	1.8
	$22.0 \log l - 2.0 \log \lambda - 30.3$	$6.1 \leq l/\lambda < 12.8$	
(0, 10)	$14.7 \log l + 5.3 \log \lambda - 23.7$	$2.4 < l/\lambda < 12.8$	6.4
	$8.9 \log l + 11.1 \log \lambda - 20.0$	$2.4 < l/\lambda \leq 6.2$	4.5
	$22.0 \log l - 2.0 \log \lambda - 30.5$	$6.2 \leq l/\lambda < 12.8$	
(0, 15)	$15.6 \log l + 4.4 \log \lambda - 25.0$	$2.4 < l/\lambda < 12.8$	4.1
	$10.2 \log l + 9.8 \log \lambda - 21.5$	$2.4 < l/\lambda \leq 6.3$	2.5
	$21.8 \log l - 1.8 \log \lambda - 30.7$	$6.3 \leq l/\lambda < 12.8$	

The relative l/λ characteristics of the four tilt-angle distributions are shown in Figure 11. The average characteristics, in dB units, were calculated by linearly interpolating the relative fish length-normalized TS of each fish in increments of 0.01 of $\log(l/\lambda)$. The average characteristics were different among the tilt-angle distributions by up to 1 dB at small l/λ, whereas the relative normalized TS was almost the same for each tilt-angle distribution at a large l/λ. The results showed that the TS of mackerel decreased with increasing l/λ from 3 to 6 and was flat in the range of $l/\lambda > 6$.

4. Discussion

4.1. Target Strength for Estimating Abundance of Mackerel

Several equations for TS related to fish length and the acoustic wavelength of mackerel for each tilt-angle distribution were derived from the results of the broadband TS measurements. The b_{20} values at a frequency of 38 kHz, which are commonly used for acoustic surveys of swim bladder fish, were −66.7 to −68.1 dB, which agreed with the modeled values (Table 4). These values were included in the range of −65.8 to −73.5 dB as estimated by previous studies [13–16,43] (Table 6). Lee and Shin [44] obtained similar b_{20} values of −67.2 dB at 50 kHz and −69.9 dB at 75 kHz that were estimated using the ex situ approach. These values were within a 2 dB difference from those found in this study, although the range of the fish lengths used in the measurements was completely different. The results of

these two studies indicated that the b_{20} of mackerel could be shared over a wide fish length range. However, Tong et al. [14] obtained the b_{20} of −73.5 dB at 38 kHz and that of −73.8 dB at 70 kHz using the KRM model, which were 6.6–6.7 dB lower than the values determined in this study. This discrepancy was likely caused by the difference in the swim bladder condition, because the acoustic backscattering from a swim bladder usually contributes more than 90% to the TS of fish with a swim bladder [45]. Comparing the two studies in terms of the ratio of swim bladder length to fish length, our samples had a relatively larger ratio, although the range of fish lengths was similar. Therefore, the size difference in the swim bladder was the most probable cause of this discrepancy.

Table 6. List of coefficients for TS equations related to fish length published in previous studies.

Frequency (kHz)	Method (Angle Distribution)	Slope *a*	Intercept *b*	b_{20}	Fish Length (cm)	Reference
38	Model (−5, 15)	11.4	−54.4	−66.0	15.4–26.2	Park et al., 2022 [13]
	Model (−5, 10)	23.6	−77.9	−73.5	13.0–22.2	Tong et al., 2022 [14]
	Model (3, 4)	40.4	−92.4	−65.8	14.8–26.9	Zhu et al., 2024 [15]
	Free Swimming (−1.2, 11.5)	27.4	−77.9	−67.9	17.4–34.0	Zhu et al., 2024 [16]
	In situ			−71.0	26–30	Gutiérrez et al., 1998 [43]
50	Ex situ (−5, 15)	27.9	−79.5	−67.2	26.2–38.3	Lee and Shin, 2005 [44]
70	Model (−5, 15)	7.2	−49.2	−66.5	15.4–26.2	Park et al., 2022 [13]
	Model (−5, 10)	24.9	−79.7	−73.8	13.0–22.2	Tong et al., 2022 [14]
	Model (3, 4)	19.4	−64.5	−65.3	14.8–26.9	Zhu et al., 2024 [15]
75	Ex situ (−5, 15)	28.6	−83.2	−69.9	26.2–38.3	Lee and Shin, 2005 [44]

The b_{20} is a simple parameter for estimating the TS. However, the slopes and intercepts of the regression lines best fitted for the relationship between TS and fish length varied with frequency (Figure 9). These results imply that the b_{20} values are not appropriate for estimating the TS of mackerel in cases where the slope is significantly different from a = 20. In particular, the estimation error can be larger if the range of fish lengths is not close to the average length used in this study. Dorsal-aspect TS mainly varies with frequency, tilt angle, and fish size (or swim bladder size), and we need to understand the relationship between the factors to estimate TS correctly. The idea of using the equation derived from the l/λ characteristics of the normalized TS can express the dependence on both fish length and frequency and may improve the TS estimation. The characteristics of fish length-normalized TS should be incorporated into the estimations of TS. The l/λ characteristics of the fish length-normalized TS obviously changed l/λ = 6.1 to 6.3, owing to the frequency dependence (Figure 10). The pair of regression equations for the range of l/λ was proposed by Love [18] as $TS = 15.8\log L + 0.42\log\lambda - 32.0$ (L/λ is 0.7 to 14) and $TS = 27.5\log L - 0.75\log\lambda - 45.4$ (L/λ is 14 to 90), where L is the fish length in meters. Note that the regression lines were obtained by integrating the maximum TSs of several species.

In this study, the TS values were estimated using four assumptions regarding the tilt-angle distributions. The variance in the tilt-angle distribution had a slight effect on the normalized TS in the small l/λ range, whereas the difference among the distributions was larger for a large l/λ. The results indicated that the normalized TS varied at high frequencies or for large fish lengths. This was caused by the frequency and size dependence of the TS pattern with tilt angle, which was more complicated at high frequencies or large fish lengths, including sharp peaks and nulls (Figures 6 and 7). Therefore, the TS in the small l/λ range was more accurate for estimating abundance. Mackerel have a wide vertical distribution and show diel vertical migration (DVM), with fish occurring in deep water during the day and moving to the surface of the water at night [26]. It should therefore be

noted that the tilt-angle distribution is not stable and varies at different times of the day. In particular, the tilt-angle distribution can tend toward fish having their head down or up during vertical movements around dawn and dusk. In these times, the TS may be lower than that in the daytime or night, assuming that the average of the tilt angle can be tens of degrees. DVM also affects swim bladder volume and shape due to the rapid change in water pressure. These times should be avoided when conducting acoustic surveys for mackerel. Unfortunately, there is no reliable data available for the tilt-angle distribution of mackerel for the estimation of TS. The broadband techniques also had potential to measure the tilt angles of fish with their high range resolution [46]. The additional data in this aspect will improve TS estimations. The angle distribution of $(-5, 15)$ was favorable for the estimation of TS because it was within the general range of the tilt-angle distribution [21].

4.2. Application in Acoustic Discrimination

Obtaining the frequency response of acoustic backscattering provided by broadband echosounders is easily available through commercial system developments. Recent studies that addressed the acoustic classification from broadband acoustic data succeeded in dividing acoustic backscattering into specific groups, including swim bladder fish [47–49]. The availability of the frequency response for classification is uncontestable, but there are still limited detailed data available on measured TSs connected with species validation. The tank experiment is a useful method for collecting basic acoustic backscattering related to some parameters for specific fish, although it has some problems in ensuring the quality of the data, such as unnatural fish conditions [4]. The datasets of broadband measurements in tanks can also be valuable for acoustic discrimination.

The relative l/λ of the normalized TS was derived to express the specific characteristics of the mackerel. Furusawa and Amakasu [27] estimated the l/λ characteristics using a prolate-spheroid model series [50] given some swim bladder types and suggested the probability of using the data for acoustic discrimination. Their results also included variations in the characteristics with tilt-angle distribution and indicated that the normalized TS was relatively flat above $l/\lambda = 5$ (noting the reference $l/\lambda = 5$ in their study). Our results also showed that the relative normalized TS was almost completely consistent among the four tilt-angle distributions in the large l/λ range (Figure 11) and could be a reliable parameter for acoustic discrimination even when measurements are conducted in situ. However, it should be noted that the characteristic varies depending on the reference l/λ, which was limited to the selection in this study owing to the individual range of l/λ.

For the discrimination among fish species with a swim bladder, the morphological difference in the swim bladder is likely to be a key parameter. The frequency response of the TS may extract its dependence. However, the TS pattern with tilt angle also depends on the size of the swim bladder, which is usually proportional to fish length We demonstrated that its effect is not negligible but indeed significant. The idea of using relative l/λ characteristics may improve the accuracy of the extraction of acoustic-specific characteristics by including size dependency. The relative l/λ characteristics of some fish species with a swim bladder were demonstrated, which showed that two or three species had different acoustic backscattering characteristics with relative l/λ while the relative frequency response of those almost overlapped (recalculated by Furusawa and Amakasu [27], using the data of Fassler et al. [51], and Pedersen and Korneliussen [52]). Although these results were obtained from a discrete frequency response, the relative l/λ characteristic provides an available index for acoustic discrimination. Additionally, no data are presently available to compare our results with those of other species to demonstrate the discriminatory power of this approach. Data collection for other swim bladder fish species is therefore needed to confirm the performance of the relative l/λ characteristics.

5. Conclusions

The dorsal-aspect TS of mackerel has been applied to other species' values in acoustic surveys and the values are considered insufficient. This study obtained the TS relationship between frequency, fish size, and tilt angle using broadband acoustic techniques. The results revealed some considerable characteristics in the TS, such as the limitation of the coefficient b_{20} due to the variation in the size dependence with frequency. The use of the l/λ characteristic may improve the application of a more precise TS for acoustic abundance estimation. TS data, with respect to a continuous and wide range of l/λ, can be easily obtained, owing to the recent widespread availability of broadband acoustic systems, and it provides useful data to discuss the detailed characteristics of TS, which is complex and variable.

The l/λ characteristic may also improve the extraction of specific characteristics that contribute to the progress in acoustic discrimination. The relative value of fish length-normalized TS with respect to l/λ derived from the measurements showed a flat response in a large l/λ range, regardless of the tilt-angle distributions for averaging the TS. As the tilt-angle distribution of fish such as mackerel may be variable in nature rather than constant, owing to their behavioral pattern, such flat characteristics should provide reliable data for acoustic discrimination.

Author Contributions: Conceptualization, K.H. and T.M.; methodology, K.H., N.Y. and Y.F.; software, K.H.; resources, N.Y. and J.Y.; investigation, N.Y. and Y.F.; formal analysis, K.H.; writing—original draft preparation, K.H.; writing—review and editing, T.M. and J.Y. All authors have read and agreed to the published version of the manuscript.

Funding: This research received no external funding.

Institutional Review Board Statement: The study was conducted by the authors having taken education and training for animal experiment of the institute (Hokkaido Univ.) and we complied the ethics.

Informed Consent Statement: Not applicable.

Data Availability Statement: The datasets presented in this article are not readily available because of time limitations. Requests to access the datasets should be directed to the authors.

Acknowledgments: This research was performed in collaboration with NIPPON KAIYO Co. Ltd. (Tokyo, Japan). The authors would like to thank the staff of the Hakodate Research Center for Fisheries and Oceans for supporting our experiments.

Conflicts of Interest: The authors declare no conflicts of interest.

References

1. Lavery, A.; Wiebe, P.H.; Stanton, T.K.; Lawson, G.L.; Benfield, M.C.; Copley, N. Determining dominant scatterers of sound in mixed zooplankton populations. *J. Acoust. Soc. Am.* **2007**, *122*, 3304–3326. [CrossRef]
2. Stanton, T.K.; Chu, D.; Jech, J.M.; Irish, J.D. New broadband methods for resonance classification and high-resolution imagery of fish with swimbladders using a modified commercial broadband echosounder. *ICES J. Mar. Sci.* **2010**, *67*, 365–378. [CrossRef]
3. Scoles, D.R.; Collette, B.B.; Graves, J.E. Global phylogeography of mackerels of the genus *Scomber*. *Fish. Bull.* **1998**, *96*, 823–842.
4. Simmonds, E.J.; MacLennan, D.N. *Fisheries Acoustics Theory and Practice*, 2nd ed.; Blackwell Science LTD.: Oxford, UK, 2005.
5. Gutiérrez, M.; Castillo, R.; Segura, M.; Peraltilla, S.; Flores, M. Trends in spatio-temporal distribution of Peruvian anchovy and other small pelagic fish biomass from 1966–2009. *Lat. Am. J. Aquat. Res.* **2012**, *40*, 633–648. [CrossRef]
6. Crone, P.R.; Hill, K.T.; Zwolinski, J.P.; Kinney, M.J. *Pacific Mackerel (Scomber japonicus) Stock Assessment for U.S. Management in the 2019–20 and 2020–21 Fishing Years*; Pacific Fishery Management Council: Portland, OR, USA, 2019.
7. Doray, M.; Boyra, G.; van der Kooij, J. *ICES Survey Protocols Manual for Acoustic Surveys Coordinated Under ICES Working Group on Acoustic and Egg Surveys for Small Pelagic Fish (WGACEGG)*, 1st ed.; International Council for the Exploration of the Sea Techniques in Marine Environmental Sciences: Copenhagen, Denmark, 2021.
8. Foote, K.G. Fish target strengths for use in echo integrator surveys. *J. Acoust. Soc. Am.* **1987**, *82*, 981–987. [CrossRef]

9. Zwolinski, J.P.; Stierhoff, K.L.; Demer, D.A. *Distribution, Biomass, and Demography of Coastal Pelagic Fishes in the California Current Ecosystem During Summer 2017 Based on Acoustic-Trawl Sampling*; U.S. Department of Commerce, NOAA Technical Memorandum NMFS-SWFSC-610: San Diego, CA, USA, 2019.
10. Lillo, S.; Cordova, J.; Paillaman, A. Target-strength measurements of hake and jack mackerel. *ICES J. Mar. Sci.* **1996**, *53*, 267–271. [CrossRef]
11. Brange, M.; Hampton, I.; Soule, M. Empirical determination of in situ target strengths of three loosely aggregated pelagic fish species. *ICES J. Mar. Sci.* **1996**, *53*, 225–232. [CrossRef]
12. Peña, H.; Foote, K.G. Modelling the target strength of *Trachurus symmetricus murphyi* based on high-resolution swimbladder morphometry using an MRI scanner. *ICES J. Mar. Sci.* **2008**, *65*, 1751–1761. [CrossRef]
13. Park, G.; Oh, W.; Oh, S.; Lee, K. Acoustic scattering characteristics of chub mackerel (*Scomber japonicus*) by KRM model. *J. Korean Soc. Fish. Ocean. Technol.* **2022**, *58*, 32–38. [CrossRef]
14. Tong, J.; Xue, M.; Zhu, Z.; Wang, W.; Tian, S. Impacts of morphological characteristics on target strength of chub mackerel (*Scomber japonicus*) in the northwest Pacific Ocean. *Front. Mar. Sci.* **2022**, *9*, 856483. [CrossRef]
15. Zhu, Z.; Tong, J.; Xue, M.; Qiu, C.; Lyu, S.; Liu, B. Investigations on target strength estimation methods: A case study of chub mackerel (*Scomber japonicus*) in the Northwest Pacific Ocean. *Fishes* **2024**, *9*, 307. [CrossRef]
16. Zhu, Y.; Ito, K.; Mizutani, K.; Minami, K.; Shirakawa, H.; Kawauchi, Y.; Iwahara, Y.; Nahata, K.; Sato, N.; Seki, K.; et al. Practical target strength of free-swimming chub mackerel *Scomber japonicus*. *Fish. Sci.* **2024**, *90*, 15–27. [CrossRef]
17. Haslett, R.W.G. Acoustic backscattering cross sections of fish at three frequencies and their representation on a universal graph. *Br. J. Appl. Phys.* **1965**, *16*, 1143–1150. [CrossRef]
18. Love, R.H. Dorsal-aspect target strength of an individual fish. *J. Acoust. Soc. Am.* **1971**, *49*, 816–823. [CrossRef]
19. Foote, K.G. On representing the length dependence of acoustic target strengths of fish. *J. Fish. Res. Board Can.* **1979**, *36*, 1490–1496. [CrossRef]
20. Miyanohana, Y.; Ishii, K.; Furusawa, M. Measurements and analyses of dorsal-aspect target strength of six species of fish at four frequencies. *Rapp. P.-v. Réum. Cons. Int. Explor. Mer.* **1990**, *189*, 317–324.
21. McClatchie, S.; Alsop, J.; Coombs, R.F. A re-evaluation of relationships between fish size, acoustic frequency, and target strength. *ICES J. Mar. Sci.* **1996**, *53*, 780–791. [CrossRef]
22. McClatchie, S.; Macaulay, G.J.; Coombs, R.F. A requiem for the use of 20 $\log_{10}$ length for acoustic target strength with special reference to deep-sea fishes. *ICES J. Mar. Sci.* **2003**, *60*, 419–428. [CrossRef]
23. Yan, N.; Mukai, T.; Hasegawa, K.; Yamamoto, J.; Fukuda, Y. Broadband target strength of arabesque greeling, Pacific sand lance, and pointhead flounder. *ICES J. Mar. Sci.* **2024**, *81*, 195–203. [CrossRef]
24. Lavery, A.; Bassett, C.; Lawson, G.L.; Jech, J.M. Exploiting signal processing approaches for broadband echosounders. *ICES J. Mar. Sci.* **2017**, *74*, 2262–2275. [CrossRef]
25. Bassett, C.; De Robertis, A.; Wilson, C.D. Broadband echosounder measurements of the frequency response of fishes and euphausiids in the Gulf of Alaska. *ICES J. Mar. Sci.* **2018**, *75*, 1131–1142. [CrossRef]
26. Yasuda, T.; Nagano, N.; Kitano, H. Diel vertical migration of chub mackerel: Preliminary evidence from a biologging study. *Mar. Ecol. Prog. Ser.* **2018**, *598*, 147–151. [CrossRef]
27. Furusawa, M.; Amakasu, K. Proposal to use fish-length-to-wavelength ratio characteristics of backscattering from fish for species identification. *J. Mar. Acoust. Soc. Jpn.* **2018**, *45*, 183–196. [CrossRef]
28. Korneliussen, R.J.; Ona, E. An operational system for processing and visualizing multi-frequency acoustic data. *ICES J. Mar. Sci.* **2002**, *59*, 293–313. [CrossRef]
29. Horne, J.K. Acoustic approaches to remote species identification: A review. *Fish. Oceanogr.* **2000**, *9*, 356–371. [CrossRef]
30. De Robertis, A.; McKelvey, D.R.; Ressler, P.H. Development and application of an empirical multifrequency method for backscatter classification. *Can. J. Fish. Aquat. Sci.* **2010**, *67*, 1459–1474. [CrossRef]
31. Amakasu, K.; Mishima, Y.; Sasakura, T.; Mukai, T.; Sawada, K. Application of multilayer piezoelectric actuators to broadband backscattering measurements of aquatic animals. *J. Marine Acoust. Soc. Jpn.* **2013**, *40*, 126–137. [CrossRef]
32. Demer, D.A.; Andersen, L.N.; Bassett, C.; Berger, L.; Chu, D.; Condiotty, J.; Cutter, G.R.; Hutton, B.; Korneliussen, R.; Bouffant, N.L.; et al. *Evaluation of a Wideband Echosounder for Fisheries and Marine Ecosystem Science*; International Council for the Exploration of the Sea Cooperative Research Report 336; ICES: Copenhagen, Denmark, 2017.
33. Clay, C.S.; Medwin, H. *Acoustical Oceanography: Principles and Applications*; Wiley-Interscience: New York, NY, USA, 1977.
34. Foote, K.G.; Knudsen, H.P.; Vestnes, G.; MacLennan, D.N.; Simmonds, E.J. *Calibration of Acoustic Instruments for Fish Density Estimation: A Practical Guide*; International Council for the Exploration of the Sea Cooperative Research Report 144; ICES: Copenhagen, Denmark, 1987.
35. Chu, D.; Stanton, T.K. Application of pulse compression techniques to broadband acoustic scattering by live individual zooplankton. *J. Acoust. Soc. Am.* **1998**, *104*, 39–55. [CrossRef]

36. Ehrenberg, J.E.; Torkelson, T.C. FM slide (chirp) signals: A technique for significantly improving the signal-to-noise performance in hydroacoustic assessment systems. *Fish. Res.* **2000**, *47*, 193–199. [CrossRef]
37. Stanton, T.K.; Chu, D. Calibration of broadband active systems using a single standard spherical target. *J. Acoust. Soc. Am.* **2008**, *124*, 128–136. [CrossRef] [PubMed]
38. Clay, C.S.; Horne, J.K. Acoustic models of fish: The Atlantic cod (*Gadus morhua*). *J. Acoust. Soc. Am.* **1994**, *96*, 1661–1668. [CrossRef]
39. Gauthier, S.; Horne, J.K. Acoustic characteristics of forage fish species in the Gulf of Alaska and Bering Sea based on Kirchhoff-approximation models. *Can. J. Fish. Aquat. Sci.* **2004**, *61*, 1839–1850. [CrossRef]
40. Medwin, H. Speed of sound in water: A simple equation for realistic parameters. *J. Acoust. Soc. Am.* **1975**, *58*, 1318–1319. [CrossRef]
41. Mackenzie, K.V. Nine-term equation for sound speed in the oceans. *J. Acoust. Soc. Am.* **1981**, *70*, 807–812. [CrossRef]
42. Foote, K.G. Averaging of fish target strength functions. *J. Acoust. Soc. Am.* **1980**, *67*, 504–515. [CrossRef]
43. Gutiérrez, M.; MacLennan, D.N. Resultados preliminares de las mediciones de fuerza de blanco in situ de las principales especies pelágicas. Crucero bic Humboldt 9803–05 de Tumbes a tacna. *Inf. Inst. Mar. Perú.* **1998**, *135*, 16–19.
44. Lee, D.J.; Shin, H.-I. Construction of a data bank for acoustic target strength with fish species, length and acoustic frequency for measuring fish size distribution. *J. Korean Fish. Soc.* **2005**, *38*, 265–275.
45. Foote, K.G. Importance of the swimbladder in acoustic scattering by fish: A comparison of gadoid and mackerel target strengths. *J. Acoust. Soc. Am.* **1980**, *67*, 2084–2089. [CrossRef]
46. Stanton, K.; Reeder, D.B.; Jech, J.M. Inferring fish orientation from broadband-acoustic echoes. *ICES J. Mar. Sci.* **2003**, *60*, 524–531. [CrossRef]
47. Benoit-Bird, K.J.; Waluk, C.M. Exploring the promise of broadband fisheries echosounders for species discrimination with quantitative assessment of data processing effects. *J. Acoust. Soc. Am.* **2020**, *147*, 411–427. [CrossRef]
48. Gugele, S.M.; Widmer, M.; Baer, J.; DeWeber, J.T.; Balk, H.; Brinker, A. Differentiation of two swim bladdered fish species using next generation wideband hydroacoustics. *Sci. Rep.* **2022**, *11*, 10520. [CrossRef] [PubMed]
49. Roa, C.; Pedersen, G.; Bollinger, M.; Taylor, C.; Boswell, K.M. Taxonomical classification of reef fish with broadband backscattering models and machine learning approaches. *J. Acoust. Soc. Am.* **2022**, *152*, 1020–1034. [CrossRef] [PubMed]
50. Furusawa, M. Prolate spheroidal models for predicting general trends of fish target strength. *J. Acoust. Soc. Jpn.* **1988**, *9*, 13–24. [CrossRef]
51. Fässler, S.M.M.; Santos, R.; García-Núñez, N.; Fernandes, P.G. Multifrequency backscattering properties of Atlantic herring (*Clupea harengus*) and Norway pout (*Trisopterus esmarkii*). *Can. J. Fish. Aquat. Sci.* **2007**, *64*, 362–374. [CrossRef]
52. Pedersen, G.; Korneliussen, R.J. The relative frequency response derived from individually separated targets of northeast Arctic cod (*Gadus morhua*), saithe (*Pollachius virens*), and Norway pout (*Trisopterus esmarkii*). *ICES J. Mar. Sci.* **2009**, *66*, 1149–1154. [CrossRef]